scientific reports

Check for updates

OPEN

Brain-derived microvesicles induce activation of aspirin-treated platelets via the PLC/PKC pathway

Yi-fan He[1], Jia-cheng Zhang[2], Yuan-zhi Wang[2], Xiao-chun Li[2], Rui-ting Zhao[4], Yi-dan Gou[2], Heng-jie Yuan[3]✉ & Ye Tian[2]✉

Aspirin (Asp) therapy reduces the risk of arterial thrombotic events. However, aspirin-related adverse effects, particularly cerebral hemorrhage with its high mortality and disability rates, remain a significant concern. Interestingly, long-term antiplatelet therapy does not appear to exacerbate bleeding severity in patients with hemorrhagic cerebrovascular disease, suggesting potential compensatory mechanisms inducing platelet activation post-hemorrhage. Brain-derived microvesicles (BDMVs) have been implicated in platelet activation, although the underlying molecular mechanisms are unclear. This study employed flow cytometry (FCM), ELISA, and hopping probe ion conductance microscopy (HPICM) to demonstrate that BDMVs significantly activate and induce morphological changes in aspirin-treated platelets. We discovered the presence of cyclooxygenase-1 (COX-1) on BDMVs. Then, the phosphorylated proteomics was used to analyze the effect of BDMVs on aspirin-treated platelet quantitatively and validate the involvement of several signaling molecules. Biological validation showed that BDMVs increased phospholipase C (PLC), protein kinase C (PKC) and Akt phosphorylation. We also used PLC inhibitor U73122 to treat BDMV-intervened platelet and found reduced phosphorylation of the downstream signaling molecule PKC. These findings suggest that COX-1 within BDMVs may partially counteract the inhibitory effect of aspirin on platelets. Furthermore, BDMVs, combined with arachidonic acid (AA), activate aspirin-treated platelets and suggest the involvement of the PLC/PKC pathway. This study provides a theoretical basis for the early treatment of patients with clinical aspirin-related cerebral hemorrhage.

Keywords Platelet, Brain-derived microvesicles, Aspirin, Phosphoproteomics, PLC/PKC pathway

The aging population in modern society has increased the incidence of cardiovascular disease yearly, and cardiovascular patients need to take long-term antithrombotic drugs to prevent acute thrombotic events. Aspirin is the most commonly used antiplatelet drugs[1]. It acetylates platelet-rich cyclooxygenase 1 (COX-1), which prevents arachidonic acid (AA) from being converted to thromboxane A2 (TXA2) and reduces TXA2 synthesis. Aspirin exerts an antiplatelet effect to prevent arterial thrombosis in patients with cardiovascular disease[2]. As aspirin has become more widespread, its adverse effects have gradually increased. Among them, cerebral hemorrhage has a high mortality and disability rate, which poses a great danger to the life of patients and the stability of society[3,4]. Cerebral hemorrhage is a non-traumatic bleeding in the brain parenchyma. The causes of morbidity are often associated with hyperlipidemia, diabetes, hypertension, anticoagulation, antiplatelet or thrombolytic therapy, leukemia, emotional stress, and overexertion[5]. However, studies have shown that previous long-term application of antiplatelet agents does not cause increased bleeding in patients with hemorrhagic cerebrovascular disease, leading to more severe consequences[6–8]. There may be some mechanism to induce platelet activation after cerebral hemorrhage and improve the bleeding status of patients.

Recently, numerous studies have identified extracellular vesicles (EVs) as a trigger and marker for deep vein thrombosis[9], cardiovascular disease[10], cancer[11], pre-thrombotic pregnancy complication[12], and post-traumatic state hypercoagulation[13,14]. And it has been shown that patients with hemorrhagic cerebrovascular disease have varying degrees of increased EVs in peripheral blood[15]. EVs are small membranous vesicles released

[1]Department of Pharmacy, Hebei General Hospital, Shijiazhuang 050051, Hebei, China. [2]Department of Neurosurgery, Tianjin Neurological Institute, Tianjin Medical University General Hospital, Tianjin 300052, China. [3]Department of Pharmacy, Tianjin Medical University General Hospital, Tianjin 300052, China. [4]Department of Pharmacy, Tianjin Medical University General Hospital Airport Hospital, Tianjin 300308, China. ✉email: hengjieyuan@tmu.edu.cn; tianye030710@163.com

from cells into the extracellular matrix and are involved in cell communication, cell migration, angiogenesis, and tumor cell growth. They are widely present in various body fluids and cell supernatants and carry several essential signaling molecules (e.g., DNA, mRNA, microRNA, lncRNA)[16]. The study of EV-related functions has become a research hotspot and is expected to play a role in the early diagnosis of many diseases. Depending on the diameter and mode of occurrence, EVs can be divided into four subgroups: exosomes (30–150 nm in diameter), microvesicles (100–1000 nm in diameter), apoptotic bodies (100–5000 nm in diameter), and oncosomes (1–10 μm in diameter)[17]. Microvesicles (MVs), as a subtype of EVs, are cellular debris produced by the outward outgrowth and division of the plasma membrane of different cell types (e.g., endothelial cells, leukocytes, platelets) and are usually released into the extracellular environment upon cell activation, necrosis or apoptosis[18–20]. MVs may also be triggered to shed due to inflammatory responses, coagulation or complement system activation, and shear stress in the circulation. By fusing with the cell membrane of the recipient cell, MVs transfer bioactive molecules into the target cell to perform physiological and pathological functions[21]. In the hematological system, MVs cause vascular inflammation, thrombosis, and calcification through the proteins they carry[22]. In the central nervous system, MVs exert dual roles, supporting neuronal development and repair while also promoting apoptosis and coagulation[23]. Our group previously demonstrated that when the brain is stimulated such as traumatic brain injury, apoptotic neuronal cells produce a large number of brain-derived microvesicles (BDMVs) that express abundant phosphatidylserine (PS) and tissue factor (TF) on their surface. Further studies revealed that BDMVs could act synergistically with platelets to open the blood–brain barrier. BDMVs can cross the open blood-brain barrier into the injured blood vessels and bind to and activate platelets[24,25]. We therefore hypothesized that BDMVs generated during cerebral hemorrhage activate platelets, potentially overcoming aspirin-induced inhibition.

In this study, we selected volunteers taking long-term aspirin to specifically explore the possible causes of platelet changes resulting from BDMVs by flow cytometry (FCM), ELISA, and hopping probe ion conductance microscopy (HPICM). We further explored the platelet activation mechanism using phosphoproteomes and Western Blot. In recent years, the successful application of mass spectrometry-based proteomics and the biological relevance of phosphorylated proteins have made possible the detailed study of phosphoproteomes[26], and phosphoproteomics techniques have become an important tool for studying cellular signaling networks[27]. This study is the first to identify differentially expressed phosphorylated proteins in BDMV-intervened platelets by using quantitative proteomics techniques. We also perform functional annotation and enrichment analysis of differentially expressed proteins. Interestingly, a large number of differentially expressed phosphorylated peptides and proteins were identified. Then we discovered the possible signaling pathway of platelet activation by BDMVs through Western Blot and the action of inhibitor U73122, which broadened our ideas further to investigate the mechanism of platelet activation by BDMVs and provided a theoretical basis for the early treatment of patients with clinical aspirin-related cerebral hemorrhage.

Methods

Ethical approval

The experimental protocol was approved by the Tianjin Medical University General Hospital. The care and use of animals were approved by the Animal Ethical Committee of the Tianjin Medical University General Hospital (Lot No.: IRB2021-DWFL-154). This research was done in compliance with the ARRIVE guidelines and regulations (https://arriveguidelines.org). All national and institutional guidelines for animal care and use have been followed throughout the study procedures. All individuals enrolled in this study signed informed consent forms. All methods were carried out in accordance with relevant guidelines and regulations.

BDMVs extraction, characterization, and quantification

Male C57BL6/J mice (8–10 weeks old and 22–25 g; Beijing HFK Biotechnology Co., Ltd, China) were housed under controlled conditions with a 12 h light-dark cycle. Water and food are unlimited. They were allowed to acclimate to the new environment for at least 1 week. During the procedure, the mice were anesthetized (2% inhaled isoflurane) and transcardially perfused with 100 mL 4 °C phosphate buffered saline (PBS). Fresh brain tissue was removed and immediately placed in centrifuge tubes on ice. According to the previous method[28], BDMVs were extracted using papain (Solarbio, Beijing) digestion and three-step centrifugation. The precipitate was resuspended with 300 μL sterile PBS to obtain BDMV suspension.

BDMVs were characterized by transmission electron microscopy (TEM; Hitachi, HT7800). Then, the extracted BDMVs were labeled, tested for positivity, and quantified by FCM. FCM analysis of cell surface glial fibrillary acidic protein (GFAP) and Annexin V binding was performed as previously described[24]. Briefly, a comprehensive six-tube panel was established for each experiment to ensure accurate gating, fluorescence compensation, and specificity controls: the experimental sample (Tube 1: double-stained for GFAP and Annexin V); single-stained controls (Tubes 2 and 4: containing only the Alexa Fluor® 488-conjugated anti-GFAP antibody or phycoerythrin (PE)-Annexin V, respectively, for compensation and threshold setting); an isotype control (Tube 3: fluorescein isothiocyanate (FITC)-IgG); an unstained BDMV control (Tube 5) to assess autofluorescence; and a buffer-only control (Tube 6) to confirm fluidic cleanliness. BDMVs were resuspended in Annexin V binding buffer containing 1.8 mM calcium. Each tube received a standardized volume of BDMV suspension and was stained with the corresponding antibodies as specified in the panel above: Alexa Fluor® 488-conjugated mouse anti-human GFAP monoclonal antibody (53-9892-82, Affymetrix eBioscience Inc.) and PE-conjugated Annexin V (560930, Becton, Dickinson and Company). After incubation at room temperature in the dark for 30 min, the reaction was stopped by adding buffer to a total volume of 500 μL. Immediately prior to analysis, Accucount Ultra rainbow Fluorescent Particles (73-ACURFP-38-5, Spherotech) were run to calibrate the instrument and define the size gate for particles. Samples were acquired on a BD FACSCanto II flow cytometer (Becton, Dickinson and Company, NJ, USA). A minimum of 100,000 events within the predefined

"vesicle gate" (based on FSC/SSC compared to beads and unstained control) were recorded. The double-positive (GFAP+/Annexin V+) population was identified based on fluorescence thresholds established from the single-stained and unstained controls (Tubes 4, 2, and 5). Next, the NanoSight300 nanoparticle tracking analyzer (NTA, Malvern Panalytical Ltd, UK) was used to detect the size and distribution.

Blood sample collection

All healthy volunteers enrolled were required to have not taken any medication. We also recruited volunteers who had taken aspirin for at least two weeks. Volunteers taking antiplatelet drugs other than aspirin, those with a history of gastrointestinal bleeding or hematologic disorders, and pregnant individuals were excluded. Blood sampling was performed by professional nurses via venipuncture with a large-gauge needle, using 3.2% sodium citrate anticoagulation tubes. No additional inhibitors of platelet activation (e.g., apyrase or prostaglandin E1) were used. Platelet-rich plasma (PRP) was prepared by centrifugation at 150 g for 15 min at room temperature using a swing-bucket rotor with controlled acceleration and no brake to ensure minimal pre-activation. Experiments were completed within 4 h of blood draw to maintain platelet responsiveness. The remaining aspirin-user PRP was divided into four groups: the Asp-control group, the Asp-BDMV group (BDMVs added), the Asp-AA group (AA added), and the Asp-BDMV + AA group (BDMVs and AA added). Prior to all experiments, platelet responsiveness was verified for each donor sample to confirm effective aspirin inhibition. PRP was stimulated with AA (final concentration 0.5 mg/mL) and ADP (final concentration 5 μM). Only samples exhibiting < 50% aggregation with AA and < 80% aggregation with ADP can proceed to further experiments. This stringent criterion ensured that all platelets used in subsequent BDMV intervention experiments were in a consistently inhibited state, reflecting the intended pharmacological effect of aspirin therapy.

Flow cytometry analysis of P-selectin expression

Platelet glycoproteins (GP), such as CD41, CD61 (GPIIIA), CD42b, and CD62p (P-selectin), not only mediate essential platelet functions such as adhesion and aggregation, but also serve as critical markers for assessing platelet activation, with CD62p (P-selectin) being a well-established activation marker. CD61 is a platelet-specific marker expressed on the surface of both resting and activated platelets[29]. P-selectin/CD62p is often used to detect platelet activation because is abundantly expressed in activated platelets[30]. The surface expression of platelet receptors was determined by FCM using the following monoclonal antibodies: anti-CD61, anti-CD62p (Becton, Dickinson and Company, NJ, USA). First, 50 μL PRP was mixed with BDMVs, and the reaction was carried out with or without AA (final concentration 250 μg/mL, Helena Agri-Enterprises, LLC., TN, USA). Samples were then stained with FITC-labeled anti-CD61 and PE-labeled anti-CD62p for 20 min at room temperature in the dark. Prepared samples were analyzed on a FACScan FCM (Becton, Dickinson and Company, NJ, USA). A minimum of 100,000 platelets was collected per sample. P-selectin was expressed as percent positive cells as previously described[31]. It should be noted that a separate isotype control was not included in this experiment. The gate for CD62p-positive cells was set based on the clear fluorescence shift observed in activated samples compared to the low fluorescence signal of the unstimulated (Asp-control) platelet population, which served as the internal reference for background staining.

Measurement of TXA2 by enzyme-linked immunosorbent assay

The amount of change in the platelet activation secretion TXA2 was examined to illustrate the effect of BDMVs on platelet activation. Because of the instability of TXA2, thromboxane B2 (the stable metabolite of TXA2) ELISA kit (ab133022, Abcam) was used according to the manufacturer's recommendation. After BDMVs were added to plasma and incubated for 30 min at room temperature, the reaction was carried out with or without AA for 2 min. Then, the supernatant was retained by centrifugation at 3000 g for 20 min. The supernatant was stored at – 80 °C for subsequent analysis.

Dynamic platelet morphology assessment by HPICM

We applied non-contact HPICM to observe the dynamic morphology of platelets during 1 h[32]. Platelet was bound to fibrinogen (1 mg/mL, bs-1240P, Beijing Bioss Biotechnology Co., Ltd) on the polystyrene cell culture dishes (Corning, USA) for 30 min, and then unbound platelet was washed off with PBS and L15 medium (Invitrogen Gibco, NY, USA). The platelet of each group was scanned and final images were produced by using ScanIC Image Viewer version 1.0 (Ionscope, Cambridge, UK).

Platelet aggregation analysis

Platelet aggregation was measured using an AggRAM (Helena Agri-Enterprises, LLC., TN, USA). Platelet aggregation was expressed as the maximum percentage change in light transmittance, with platelet-poor plasma (PPP) set as 100% and PRP set as 0%. AA was used as the agonist. To assess BDMV effects, PRP was pre-incubated with various BDMV concentrations at room temperature for 30 min prior to AA addition. The test was performed according to the instructions.

Phosphorylated proteomics analysis

We selected 9 healthy volunteers and 12 aspirin users, and collected 5 mL blood intravenously. Then, PRP was obtained by centrifugation. The PRP of healthy volunteers was added AA, described as the Nor-AA group. The PRP of aspirin users was divided into two groups: the Asp-AA group and the Asp-BDMV + AA group. We then extracted the protein from the platelet pellet obtained by centrifugation for subsequent phosphorylation proteomics assay. The protein was extracted by SDT (4% (w/v) SDS, 100 mM Tris/HCl pH 7.6, 0.1 M DTT) lysis, and then protein quantification was performed by BCA method.

Each sample was separated using the high performance liquid chromatography (HPLC) liquid phase system nanoelute at nanoliter flow rate and analyzed by mass spectrometry using a timsTOF Pro mass spectrometer. The data acquisition mode was used in the parallel accumulation–serial fragmentation (PASEF) mode. The raw mass spectrometry data were analyzed using MaxQuant software (v1.5.3.17)[33]. Peptides and proteins were identified according to Maxquant's own algorithm and the Uniprot database to give relative quantitative information (Intensity)[34]. Differential peptides and proteins were filtered to draw clusters, volcano plots and conduct Gene Ontology (GO) analysis, Kyoto Encyclopedia of Genes and Genomes (KEGG) pathway analysis, and the analysis conserved motifs of related genes.

Western blot

First, we used anti-COX-1 antibody (ab109025, Abcam, 1:1000) to test whether COX-1 was contained in the BDMVs and brain tissue. We also extracted protein from C57BL6/J mice hair as a negative control. Then, we detected differentially expressed AKT1 (phospho S129) proteins in each group to verify the result of phosphoproteomics. U73122 (10 μM, S8011, Selleck) is a potent phospholipase C (PLC) inhibitor. U73122 and PRP were reacted for 30 min, followed by the addition of BDMVs and AA. Platelet protein extraction was performed on another 6 aspirin users and 6 healthy volunteers. Equal amounts of protein were subjected to SDS-PAGE. The sources of antibodies and dilutions used were as follows: Akt antibody (9272, Cell Signaling Technology, 1:1000), recombinant anti-AKT1 (phospho S129) antibody [EPR6150] (ab133458, Abcam, 1:1000), phospho-(Ser) PKC substrate antibody (2261, Cell Signaling Technology, 1:1000), and mouse anti-GAPDH (Beijing Zhongshan Jinqiao Technology Co., Ltd, 1:5000), which was used as an internal control.

Statistical analysis

FCM data were analyzed using FlowJo. Western blot band intensities were quantified using Image J. Statistical analyses were performed using Graphpad Prism 9.3.0. (San Diego, CA, USA). Normality and Lognormality Test was used to test normality. Comparisons between two groups used Student's t-test. Multiple group comparisons used one-way ANOVA. Quantitative results were expressed as mean±standard error of the mean (mean ± SEM). $P < 0.05$ was considered statistically significant.

Results

BDMVs characterization

TEM observed many BDMVs with bilayer vesicle structures (Fig. 1A). And the extracted BDMVs expressed GFAP in significant quantities by FCM, indicating that these BDMVs were of glial cell origin. However, they exist for only a small number of PS (Fig. 1B). The mean concentration of BDMVs was 7.09×10^7/μL (Fig. 1C). The NTA showed that the size was distributed between 100 and 600 nm, with two peaks between 140 and 240 nm and 290 and 420 nm. The average size was 171.1 ± 85.5 nm (Fig. 1D). The above data and images indicate that a high concentration of BDMVs was successfully extracted *in vitro* using papain digestion.

BDMV effects on platelet activation and morphology

To investigate the effects of BDMVs on aspirin-treated platelets, we first established a robust model of aspirin inhibition. All platelet samples were pre-screened and confirmed to be hypo-responsive to both AA (< 50% aggregation) and ADP (< 80% aggregation), ensuring a consistent baseline of pharmacological inhibition. The $CD62p^+$% of each group was measured (Fig. 2A). The results showed that the action of BDMVs and AA induced platelet activation. Thromboxane B2 (TXB2) concentration was no statistically significant change in the Asp-BDMV group compared with the Asp-control group. However, TXB2 concentration was apparently elevated in the Asp-BDMV + AA group (Fig. 2B). HPICM visually showed the changes in platelet morphology under different conditions (Fig. 2C). The platelet morphology in the Asp-control group was stable, and some bulging platelets slowly became more regular. Most of the platelet in the Asp-BDMV group was also tough, and only a few platelets ruptured and disappeared. In the Asp-AA group, most platelets also did not undergo dramatic morphological change. In the Asp-BDMV + AA group, almost all of the platelet changed dramatically, and finally, they ruptured and disappeared. Although BDMVs induced the expression of activation markers, they inhibited AA-induced platelet aggregation in a concentration-dependent manner (BDMVs ≈ 10^3/μL (1); BDMVs ≈ 10^4/μL (2); BDMVs ≈ 10^5/μL (3); BDMVs ≈ 10^6/μL (4)) (Fig. 2D).

Phosphoproteomics analysis of BDMV-intervened platelets

To investigate the underlying mechanisms by which BDMVs activate platelets, we conducted a non-targeted phosphoproteomic analysis (Fig. 3A). The Fig. 3B shows the quantitative differences in phosphorylated peptides between the three comparison groups. A total of 19,586 phosphorylation sites (19,496 phosphorylation sites were quantified), 7904 phosphorylated peptides (7859 phosphorylated peptides were quantified), and 2829 phosphorylated proteins (2811 phosphorylated proteins were quantified) were identified in this study (Supplementary Data). We also performed the cluster analysis and drawn the volcano plots of differentially expressed proteins (Fig. 3C–E, Supplementary Figs. 1–6).

On this basis, we compared the Asp-AA group with the Nor-AA group to look for down-regulated expression to find expression of phosphorylated proteins when platelets were not activated. We compared the Asp-BDMV + AA group with the Asp-AA group to look for up-regulated expression to identify phosphorylated proteins affected by BDMVs. We compared the Asp-BDMV + AA group with the Nor-AA group to look for up-regulated expression to find BDMVs significantly affect the pathways of platelet activation.

The GO covers three domains: biological process (BP), cellular component (CC) and molecular function (MF)[35]. In the down-regulation comparison between the Asp-AA group and the Nor-AA group (Fig. 4A), the BP that was significantly enriched mainly included protein location to posodome assembly, platelet formation,

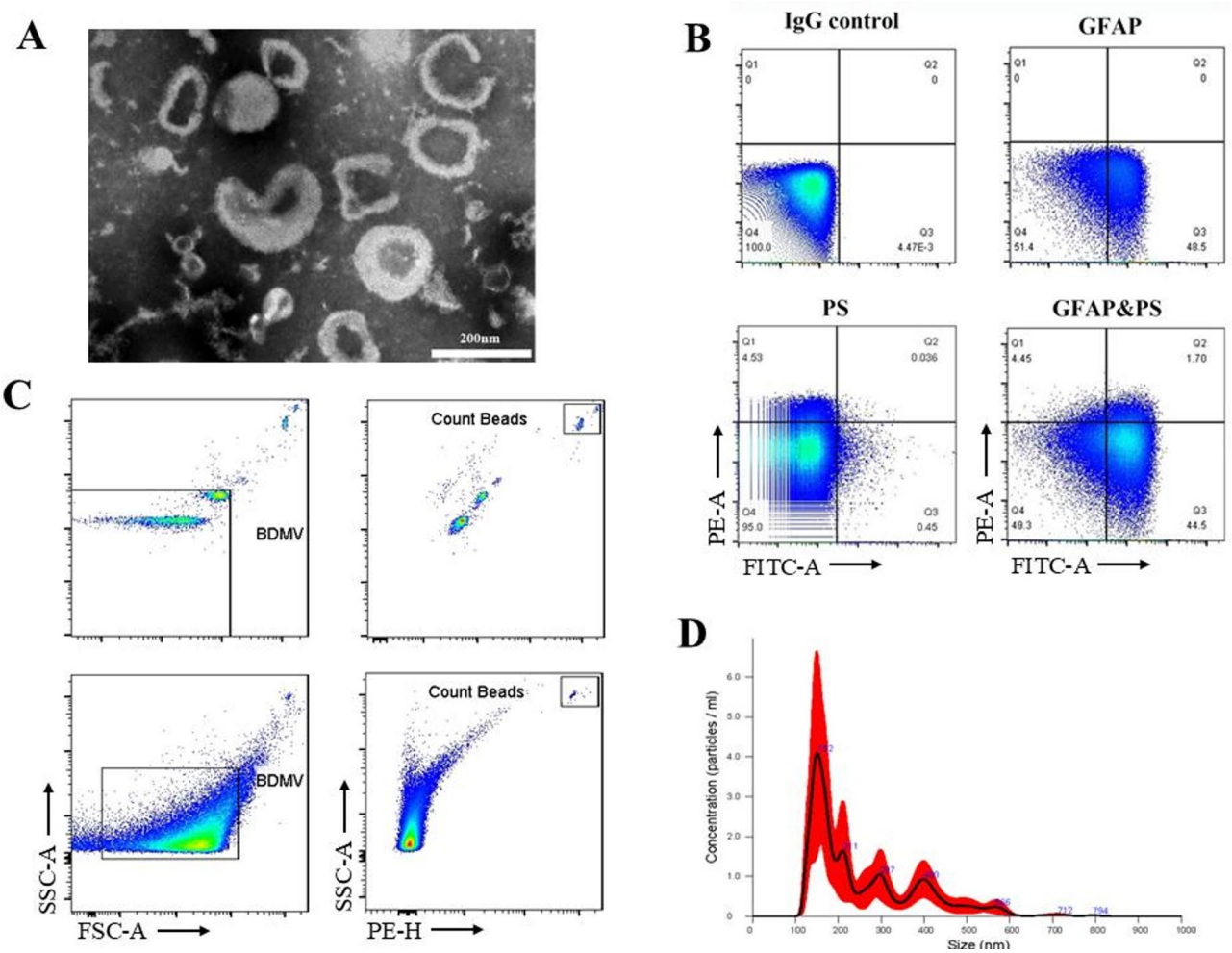

Fig. 1. Detection of BDMVs. (**A**) Representative transmission electron microscope image of BDMVs. TEM image of BDMVs with negative staining to enhance the view of membrane structures (bar=200 nm). (**B**) The expression of GFAP, PS, and both was measured for BDMVs by flow cytometry. (**C**) Quantity detection of BDMVs by flow cytometry. (**D**) The detection of BDMV size by the Nanoparticle tracking analyzer. The data represent 3 separate experiments. BDMVs, brain-derived microvesicles; GFAP, glial fibrillary acidic protein; PS, phosphatidylserine.

and platelet morphogenesis. The significantly enriched CC mainly included microtubule plus-end, podosome, platelet dense tubular network, and platelet dense granule. The MF included profilin binding, microtubule plus-end binding, calcium-dependent protein kinase C activity and protein kinase C activity. In the up-regulation comparison between the Asp-BDMV + AA group and the Asp-AA group (Fig. 4B), the BP mainly included transepithelial transport and nucleobase transport. The CC mainly included platelet dense tubular network, intracellular component, and microtubule plus-end. The MF mainly included profilin binding, calcium-dependent protein kinase C activity, protein kinase C activity, and calcium-dependent protein serine/threonine kinase activity. In the up-regulation comparison between the Asp-BDMV + AA group and the Nor-AA group (Fig. 4C), the BP mainly included positive regulation of extracellular matrix assembly and positive regulation of substrate adhesion-dependent cell spreading. The CC mainly included neuronal dense core vesicle, platelet dense tubular network, and cAMP-dependent protein kinase complex. The MF also included profilin binding, calcium-dependent protein kinase C activity, protein kinase C activity, and calcium-dependent protein serine/threonine kinase activity.

Then, we performed KEGG pathway analysis to annotate and speculate on the pathways in which differentially phosphorylated proteins may be involved. In the down-regulation comparison between the Asp-AA group and the Nor-AA group, the most significantly enriched pathway was platelet activation (Fig. 5A), where we identified that PLCβ3(S537), MLCK(S1617), Btk(S174), Akt1(S129), Talin1(T1616) and other proteins were downregulated (Fig. 5B). In the up-regulation comparison between the Asp-BDMV + AA group and the Asp-AA group, the significantly enriched pathways were glutamatergic synapse, cholinergic synapse, calcium signaling pathway and platelet activation (Fig. 5C). By comparing in Asp-BDMV + AA group and the Asp-AA group, we found that proteins which were down-regulated in Fig. 5B underwent significant up-regulation in Fig. 5D. PLCβ1(S581), MLCK(S1773), Btk(T191), Akt1(S129), Talin1(S1942) and other upregulated proteins

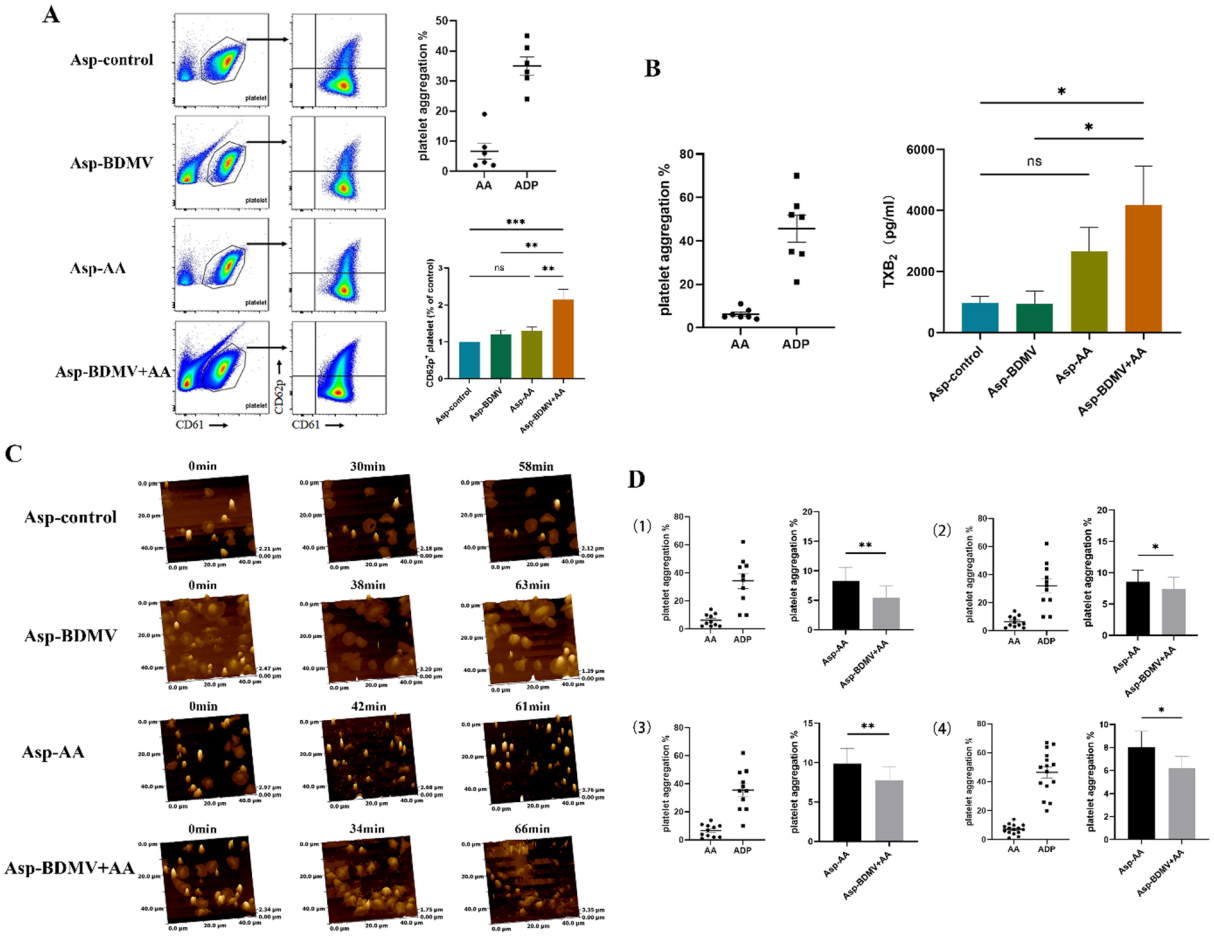

Fig. 2. BDMV effects on aspirin-treated platelet activation, morphology, and aggregation. (**A**) Flow cytometry analysis of P-selectin (CD62p) expression on platelets. The gate for CD62p-positive cells was determined by comparison with the fluorescence profile of the unstimulated Asp-control group, which defined the background level. Data are representative of 6 separate experiments. (**B**) Measurement of thromboxane B2 (TXB2) concentration by ELISA (representative of 7 separate experiments). The aggregation tracings in the upper right corner represent the pre-qualification data for the sample used in this specific experiment. (**C**) Dynamic platelet morphology assessment by HPICM over 1 h (representative of 3 separate experiments). The aggregation tracings on the left represent the pre-qualification data for the sample used in this specific experiment. (**D**) Platelet aggregation analysis in response to AA following pre-incubation with various concentrations of BDMVs (BDMVs $\approx 10^3$/μL, $n = 10$ (1); BDMVs $\approx 10^4$/μL, $n = 11$(2); BDMVs $\approx 10^5$/μL, $n = 11$(3); BDMVs $\approx 10^6$/μL, $n = 15$(4)). Results from 4 independent experiments using blood samples from different aspirin-treated platelet. Each panel displays the baseline platelet aggregation response of its respective sample to AA and ADP prior to BDMV intervention, confirming the inhibited state of the platelets. $^*p < 0.05$, $^{**}p < 0.01$, $^{***}p < 0.001$. AA, arachidonic acid; TXB2, thromboxane B2; HPICM, hopping probe ion conductance microscopy.

mostly modified at different phosphorylation sites. In the up-regulation comparison between Asp-BDMV + AA group and the Nor-AA group, the most significantly enriched pathways were also platelet activation (Fig. 5E). The phosphorylated proteins upregulated in the platelet activation pathway are shown in Fig. 5F.

To uncover the specific kinase-substrate relationships underlying the phosphoproteomic changes, we performed a motif enrichment analysis by using MEME software[36]. This analysis revealed distinct signaling signatures in different comparisons. Six phosphorylated modified peptide motifs were identified in the down-regulation comparison between the Asp-AA group and the Nor-AA group, with the highest score of 24.03 (Fig. 6A). In the up-regulation comparison between the Asp-BDMV + AA group and the Asp-AA group, two phosphorylated modified peptide motifs were identified, and the highest motif score was 16.00 (Fig. 6B). In the up-regulation comparison between the Asp-BDMV + AA group and the Nor-AA group, five phosphorylated modified peptide motifs were identified, and the highest motif score was 22.99 (Fig. 6C). Most notably, in the Asp-BDMV + AA vs. Asp-AA comparison the most significant motif featured a phosphorylated serine followed by a proline at the + 1 position ([pS]-P, Fig. 6B). This motif is a canonical target for proline-directed kinases, such as mitogen-activated protein kinases (MAPKs)[37] and cyclin-dependent kinases (CDKs), suggesting their potential activation by BDMVs. Furthermore, motifs enriched in the other comparisons were characterized

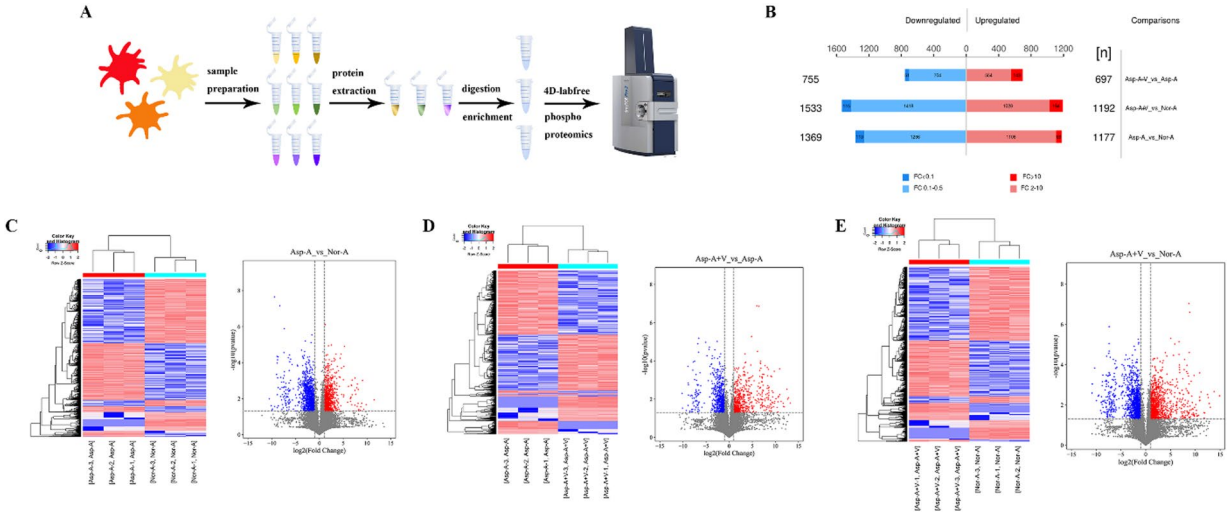

Fig. 3. Basic information about phosphorylation proteomics analysis. (**A**) Flow chart of phosphorylation proteomics analysis. (**B**) Histogram of quantitative difference results of phosphorylated peptide fragments. (**C–E**) Heat map and scatter plot in the comparison among the Asp-AA/Asp-A group and the Nor-AA/Nor-A group, the Asp-BDMV + AA/Asp-A + V group and the Asp-AA/Asp-A group, and the Asp-BDMV + AA/Asp-A + V group and the Nor-AA/Nor-A group. Red, blue, and gray clusters indicate up-, down-, and unregulated proteins, respectively. The data represent 3 separate experiments. Asp, aspirin; Nor, normal.

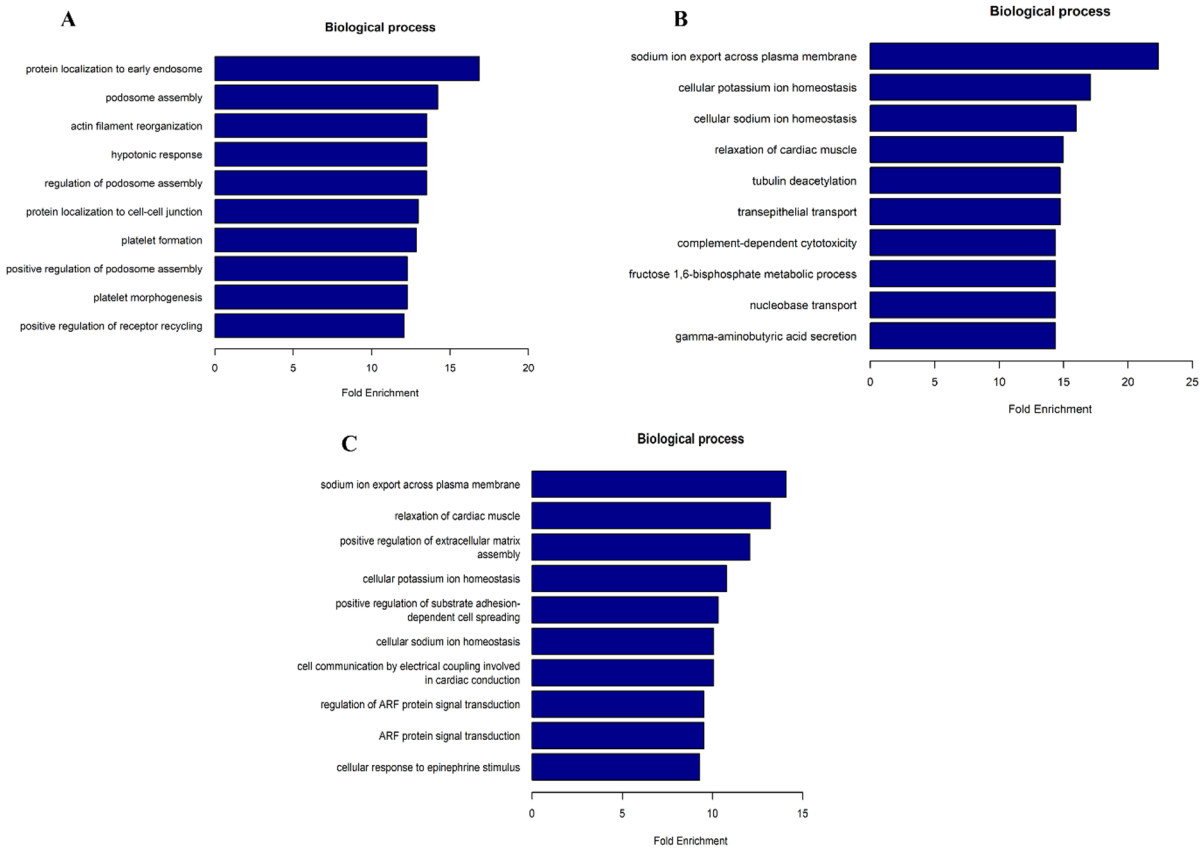

Fig. 4. GO enrichment analysis (**A**) Biological processes identified by GO enrichment analysis in the down-regulated comparison between the Asp-AA/Asp-A group and the Nor-AA/Nor-A group. (**B**) Biological processes identified by GO enrichment analysis in the up-regulated comparison between the Asp-BDMV + AA/Asp-A + V group and the Asp-AA/Asp-A group. (**C**) Biological processes identified by GO enrichment analysis in the up-regulated comparison between the Asp-BDMV + AA/Asp-A + V group and the Nor-AA/Nor-A group. GO, Gene Ontology.

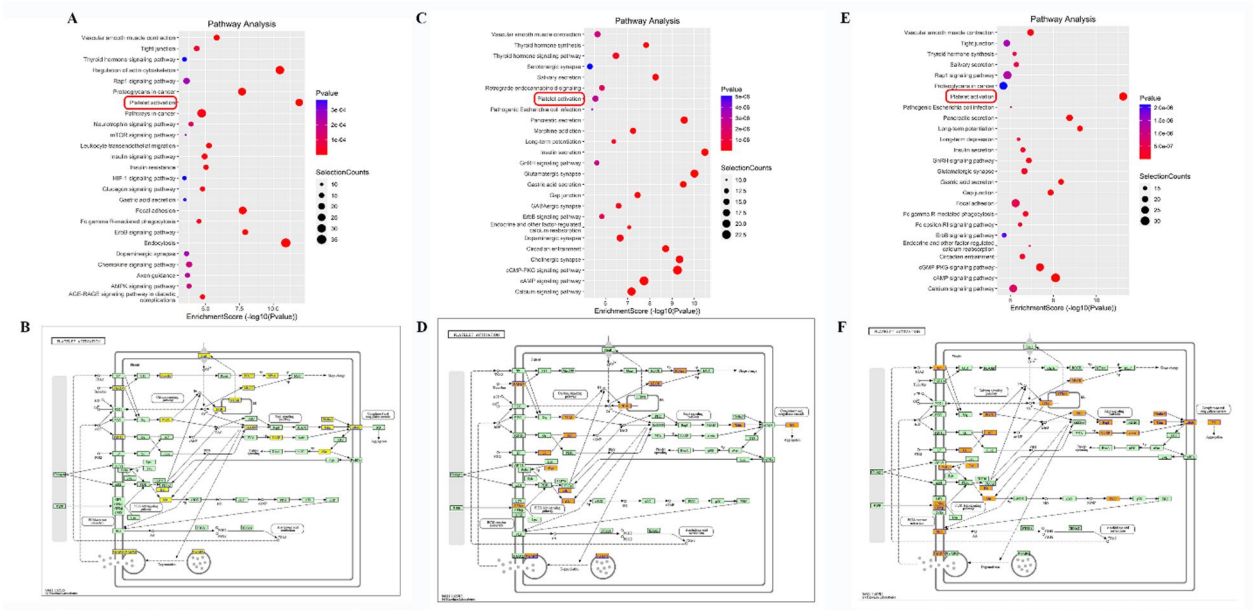

Fig. 5. KEGG pathway analysis and the platelet activation pathway (**A**) KEGG pathway analysis in the down-regulated comparison between the Asp-AA/Asp-A group and the Nor-AA/Nor-A group. (**B**) Alterations in phosphorylated proteins in the platelet activation pathway between the Asp-AA/Asp-A group and the Nor-AA/Nor-A group. (**C**) KEGG pathway analysis in the up-regulated comparison between the Asp-BDMV + AA/Asp-A + V group and the Asp-AA/Asp-A group. (**D**) Alterations in phosphorylated proteins in the platelet activation pathway between the Asp-AA/Asp-A group and the Nor-AA/Nor-A group. (**E**) KEGG pathway analysis in the up-regulated comparison between the Asp-BDMV + AA/Asp-A + V group and the Nor-AA/Nor-A group. (**F**) Alterations in phosphorylated proteins in the platelet activation pathway between the Asp-AA/Asp-A group and the Nor-AA/Nor-A group. Yellow marked nodes are associated with down enriched genes, orange marked nodes are associated with up-regulated enriched genes, and green nodes have no significance. KEGG, Kyoto Encyclopedia of Genes and Genomes.

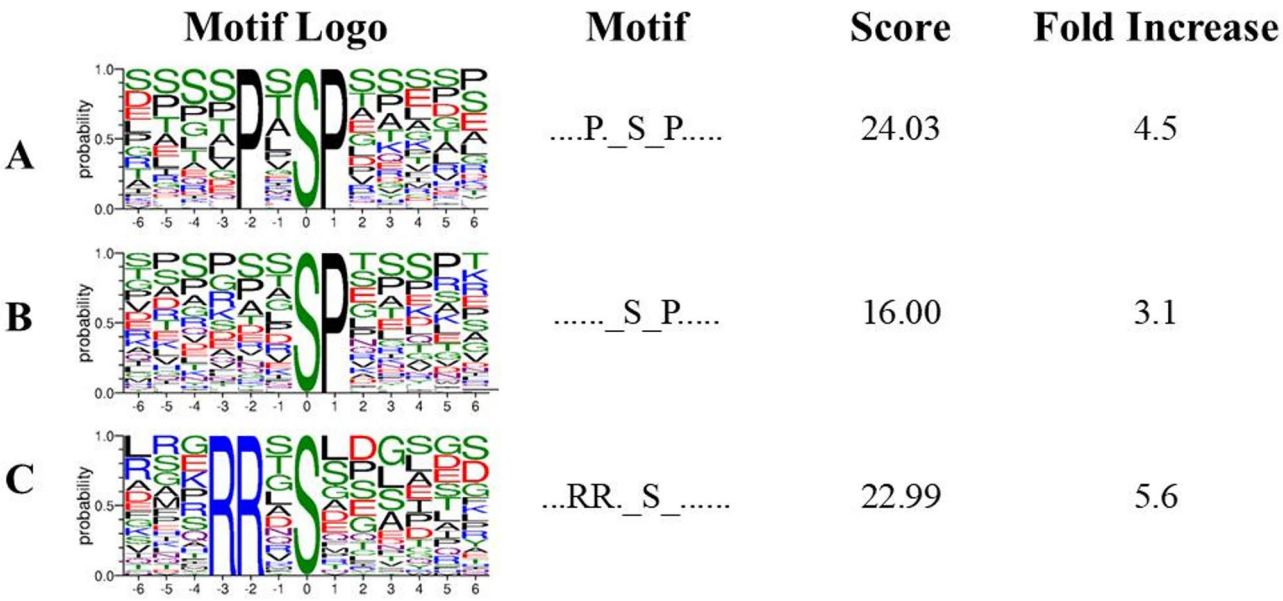

Fig. 6. Conserved phosphorylation motifs and predicted upstream kinases identified by motif enrichment analysis. (**A**) Motifs enriched in peptides down-regulated in the Asp-AA/Asp-A vs. Nor-AA/Nor-A comparison. (**B**) Motifs enriched in peptides up-regulated in the Asp-BDMV + AA/Asp-A + V vs. Asp-AA/Asp-A comparison. (**C**) Motifs enriched in peptides up-regulated in the Asp-BDMV + AA/Asp-A + V vs. Nor-AA/Nor-A group comparison. For each motif, the sequence logo is shown, and the consensus sequence and score are annotated to its right.

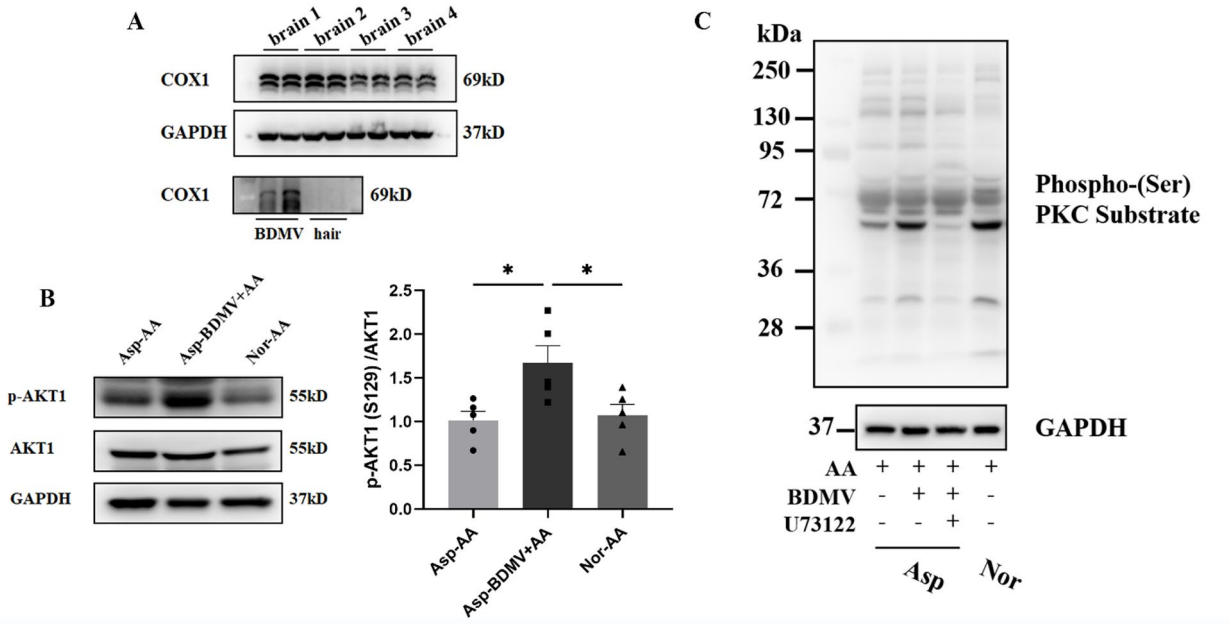

Fig. 7. Western Blot analysis. (**A**) The expression of COX-1 in brain tissue (representative of 4 separate experiments) and BDMVs (representative of 3 separate experiments). (**B**) Validation of effect of BDMVs on Akt (S129) phosphorylation in aspirin-treated platelet (representative of 5 separate experiments). (**C**) Western blot analysis of the phosphorylation PKC substrate. The data represent 6 separate experiments. Uncropped blots are in Supplementary Material. *$p < 0.05$. COX-1, cyclooxygenase 1; PKC, protein kinase C.

by basic residues (Arg/Lys) at flanking positions (Fig. 6A, C), which are typical recognition sites for basophilic kinases like protein kinase C (PKC) and protein kinase A (PKA).

Validation of the effect of BDMVs in aspirin-treated platelets

Western Blot examined the presence of COX-1 in mouse brain tissue, BDMVs, and hair. The results showed that COX-1 was detected in brain tissue and BDMVs. We selected mouse hair as a negative control group, further showing the presence of COX-1 in BDMVs (Fig. 7A).

Next, we selected antibodies with corresponding phosphorylation sites for Western Blot validation. The level of p-Akt1 (S129) was upregulated in the Asp-BDMV + AA group compared to the Asp-AA group and the Nor-AA group ($P < 0.05$), which was consistent with the results of phosphoproteomics (Fig. 7B). Phosphorylated proteomics results also found a significant effect of BDMVs on the phosphorylation of platelet PLC and PKC. To validate the proteomic findings, we employed the PLC inhibitor U73122. The results showed a significant reduction in PKC phosphorylation levels, suggesting that the PLC/PKC pathway may be involved in the BDMV-induced activation process (Fig. 7C).

Discussion

In this study, we investigated the effects of BDMVs on platelet function in aspirin-treated individuals and explored the underlying mechanisms by which BDMVs activate platelets under aspirin inhibition. Our findings provide novel insights into the complex interplay between BDMVs and platelet signaling pathways, particularly in the context of COX-1 activity and phosphoproteomic alterations.

First, we characterized BDMVs extracted via papain digestion, confirming their size, morphology, source, and concentration through TEM, NTA, and FCM. These BDMVs exhibited a bilayer membrane structure, glial origin (GFAP-positive), and PS exposure, consistent with our previous studies[24,28]. Subsequent experiments demonstrated that BDMVs, in combination with AA, induced significant platelet activation and morphological changes in aspirin-treated platelets. This activation is likely mediated through two primary mechanisms: membrane-to-membrane contact and fusion of BDMVs with platelets, leading to the delivery of bioactive cargo (e.g., proteins) into platelets, as documented in prior research on MVs[38]. Notably, platelets themselves can generate MVs[39], and platelet-derived MVs contain COX-1 and thromboxane[40], suggesting a potential role for vesicular COX-1 in platelet regulation.

COX-1 is intrinsically expressed in platelets and various tissues (e.g., blood vessels, stomach, kidneys, brain) and plays a crucial role in regulating platelet aggregation, vasoconstriction, gastric mucosa integrity, and renal blood flow[41–43]. It is also essential for AA-mediated platelet activation[44]. Aspirin inhibits COX-1, preventing the conversion of AA to TXA2 and thereby exerting an antiplatelet effect[45]. Our data suggest that BDMVs may contain functional COX-1, which could partially counteract aspirin's inhibition. The observed increase in TXB2 levels upon co-administration of BDMVs and AA supports this hypothesis, indicating that BDMV-derived COX-1 remains active and utilizes exogenous AA to generate TXA2, bypassing the aspirin blockade. However,

to fully confirm the enzymatic activity and kinetics of COX-1 within BDMVs, future studies should employ dynamic assays measuring thromboxane generation rates and COX-1-specific inhibitors to establish a direct causal relationship.

It is important to address the potential presence of non-specific cellular debris in our BDMV preparations. However, multiple lines of evidence support the enrichment of bona fide MVs: TEM revealed characteristic bilayer membranes, NTA confirmed a size distribution consistent with MVs (100–600 nm), and FCM detected positive markers for PS (Annexin V binding) and GFAP. While additional MV-specific markers would strengthen future work, the current data collectively indicate that the biological effects are attributable to BDMVs rather than non-functional debris.

A paradoxical finding emerged from our aggregation assays, where BDMVs caused a concentration-dependent inhibition of aggregation despite inducing platelet activation (as evidenced by increased P-selectin expression and morphological changes). This apparent discrepancy can be explained by the induction of a procoagulant "balloon-like" platelet phenotype, which is aggregation-incompetent but highly active in supporting coagulation[46–48]. Our HPICM data showed that platelets in the Asp-BDMV + AA group underwent dramatic, unconstrained morphological alterations, culminating in membrane disintegration and disappearance, rather than stable spreading and aggregation. This suggests that BDMVs drive platelets into an exhaustive hyperactivated state, potentially due to overwhelming calcium influx or irreversible cytoskeletal contraction. In this state, platelets may expose PS (promoting thrombin generation) but lose structural integrity required for cohesive aggregate formation[49]. Thus, the inhibition of aggregation is a direct consequence of extreme activation, shifting platelet function from aggregation to a procoagulant role, which may be relevant in cerebral hemorrhage pathophysiology.

To elucidate the signaling mechanisms underlying BDMV-induced activation, we conducted a comprehensive phosphoproteomic analysis. Protein post-translational modifications (PTMs), particularly phosphorylation, are critical regulators of platelet function, especially given the anucleate nature of platelets[50]. Thus, we examined the alterations of phosphorylated proteins in platelets by using quantitative proteomics techniques based on next-generation 4D label free ion drip mass spectrometry[34,51]. Our quantitative proteomics approach revealed widespread changes in the platelet phosphoproteome upon BDMV exposure. The Supplementary Tables 1–3 show the top 15 differentially expressed proteins. Key findings included the down-regulation of bridging integrator 2 (BIN2) in the Asp-AA group vs. the Nor-AA group, and the up-regulation of calcium/calmodulin-dependent protein kinase type II subunit alpha (CAMK2A) and protein kinase C gamma type (PRKCG) in the Asp-BDMV + AA group compared to both Asp-AA and Nor-AA groups. BIN2 loss is known to cause Ca^{2+} store release and reduced influx in response to agonists[52], while CAMK2A regulates synaptic plasticity and neurotransmitter release[53]. GO and KEGG analyses further highlighted down-regulation of platelet formation, dense granule release, and protein kinase C activity in the Asp-AA group vs. the Nor-AA group comparison, with platelet activation being the most significantly enriched pathway. Specifically, proteins such as PLCβ3 (S537), MLCK (S1617), Btk (S174), Akt1 (S129), and Talin1 (T1616) were down-regulated. In contrast, the Asp-BDMV + AA group showed up-regulation of similar proteins at different phosphorylation sites (e.g., PLCβ1 S581, MLCK S1773, Btk T191, Akt1 S129, Talin1 S1942), indicating a reversal of the aspirin-induced suppression.

Pharmacological inhibition of PLC with U73122 significantly reduced PKC phosphorylation, supporting the involvement of the PLC/PKC pathway in BDMV-mediated activation. PLC is widely distributed and activated via G proteins, playing a vital role in phosphatidy-linositol signaling[54], while PKC is a Ca^{2+}-activated serine/threonine kinase regulating gene expression, proliferation, apoptosis, and migration[55]. Thus, BDMVs likely induce platelet activation through the PLC/PKC pathway, potentially due to the presence of COX-1.

Motif analysis identified conserved phosphorylation motifs, such as basophilic motifs enriched in proline-directed kinase substrates[56], which were associated with platelet activation in the Asp-BDMV + AA group. These motifs represent binding sites for upstream kinases (e.g., PKC family), which introduce or remove phosphate groups to regulate substrate activity through conformational changes[57]. And their enrichment aligns with our functional data showing PKC pathway activation. This consistency between motif prediction and pharmacological validation strengthens the conclusion that PLC/PKC signaling is a key mechanism.

In summary, our study demonstrates that BDMVs may contain COX-1 and activate aspirin-treated platelets via the PLC/PKC pathway, as evidenced by phosphoproteomic changes and inhibitor experiments. The paradoxical activity of BDMV-derived COX-1 post-aspirin can be explained by its glial origin and compartmentalization within bilayer membranes, which may shield it from aspirin inhibition. Additionally, BDMVs rely on exogenous AA for TXA2 generation, and their effects are synergized by PLC/PKC activation. However, platelet activation is a complex process involving multiple pathways, and we cannot attribute it solely to one mechanism[58,59]. While this study provides key insights into BDMV-platelet interactions, its findings also highlight important unresolved questions. Specifically, the validation of key phosphorylation sites was hampered by limited antibody availability, and the mechanism of BDMV internalization emerged as a critical unknown. To bridge these knowledge gaps, subsequent research should leverage endocytosis inhibitors like dynasore and high-resolution imaging to definitively establish the uptake pathway and its functional necessity for PLC/PKC activation. Resolving these details will be essential for a complete mechanistic understanding of how BDMVs modulate platelet function in hemostasis and thrombosis.

Data availability

All data generated or analyzed during this study are included in this published article.

Received: 29 June 2025; Accepted: 5 February 2026
Published online: 25 March 2026

References

1. Assadian, A. et al. Aspirin resistance among long-term aspirin users after carotid endarterectomy and controls: flow cytometric measurement of aspirin-induced platelet Inhibition. *J. Vasc. Surg.* **45**, 1142–1147. https://doi.org/10.1016/j.jvs.2007.01.064 (2007). discussion 1147.
2. Roffi, M. et al. ESC Guidelines for the management of acute coronary syndromes in patients presenting without persistent ST-segment elevation: Task Force for the Management of Acute Coronary Syndromes in Patients Presenting without Persistent ST-Segment Elevation of the European Society of Cardiology (ESC). *Eur. Heart J.* **37**, 267–315. https://doi.org/10.1093/eurheartj/ehv320 (2016).
3. Global, regional, and national burden of stroke and its risk factors, 1990–2019: a systematic analysis for the global burden of disease study 2019. *Lancet Neurol.* **20**, 795–820. https://doi.org/10.1016/s1474-4422(21)00252-0 (2021).
4. Gross, B. A., Jankowitz, B. T. & Friedlander, R. M. Cerebral intraparenchymal hemorrhage: A review. *Jama* **321**, 1295–1303. https://doi.org/10.1001/jama.2019.2413 (2019).
5. Hostettler, I. C., Seiffge, D. J. & Werring, D. J. Intracerebral hemorrhage: an update on diagnosis and treatment. *Expert Rev. Neurother.* **19**, 679–694. https://doi.org/10.1080/14737175.2019.1623671 (2019).
6. Ivascu, F. A. et al. Predictors of mortality in trauma patients with intracranial hemorrhage on preinjury aspirin or clopidogrel. *J. Trauma.* **65**, 785–788. https://doi.org/10.1097/TA.0b013e3181848caa (2008).
7. Nishijima, D. K., Zehtabchi, S., Berrong, J. & Legome, E. Utility of platelet transfusion in adult patients with traumatic intracranial hemorrhage and preinjury antiplatelet use: a systematic review. *J. Trauma. Acute Care Surg.* **72**, 1658–1663. https://doi.org/10.1097/TA.0b013e318256dfc5 (2012).
8. Sansing, L. H. et al. Prior antiplatelet use does not affect hemorrhage growth or outcome after ICH. *Neurology* **72**, 1397–1402. https://doi.org/10.1212/01.wnl.0000342709.31341.88 (2009).
9. Zhou, L. et al. Microparticles: new light shed on the Understanding of venous thromboembolism. *Acta Pharmacol. Sin.* **35**, 1103–1110. https://doi.org/10.1038/aps.2014.73 (2014).
10. Schiro, A. et al. Endothelial microparticles as conveyors of information in atherosclerotic disease. *Atherosclerosis* **234**, 295–302. https://doi.org/10.1016/j.atherosclerosis.2014.03.019 (2014).
11. Geddings, J. E. & Mackman, N. Tumor-derived tissue factor-positive microparticles and venous thrombosis in cancer patients. *Blood* **122**, 1873–1880. https://doi.org/10.1182/blood-2013-04-460139 (2013).
12. Kaptan, K., Beyan, C., Ifran, A. & Pekel, A. Platelet-derived microparticle levels in women with recurrent spontaneous abortion. *Int. J. Gynaecol. Obstet.* **102**, 271–274. https://doi.org/10.1016/j.ijgo.2008.04.007 (2008).
13. Park, M. S. et al. Quantification of hypercoagulable state after blunt trauma: microparticle and thrombin generation are increased relative to injury severity, while standard markers are not. *Surgery* **151**, 831–836. https://doi.org/10.1016/j.surg.2011.12.022 (2012).
14. Booth, A. M. et al. Exosomes and HIV gag bud from endosome-like domains of the T cell plasma membrane. *J. Cell Biol.* **172**, 923–935. https://doi.org/10.1083/jcb.200508014 (2006).
15. Laso-García, F. et al. Protein content of blood-derived extracellular vesicles: an approach to the pathophysiology of cerebral hemorrhage. *Front. Cell. Neurosci.* **16**, 1058546. https://doi.org/10.3389/fncel.2022.1058546 (2022).
16. van Niel, G., D'Angelo, G. & Raposo, G. Shedding light on the cell biology of extracellular vesicles. *Nat. Rev. Mol. Cell Biol.* **19**, 213–228. https://doi.org/10.1038/nrm.2017.125 (2018).
17. Urabe, F. et al. Extracellular vesicles as biomarkers and therapeutic targets for cancer. *Am. J. Physiol. Cell Physiol.* **318**, C29–c39. https://doi.org/10.1152/ajpcell.00280.2019 (2020).
18. Ratajczak, M. Z. & Ratajczak, J. Extracellular microvesicles/exosomes: discovery, disbelief, acceptance, and the future? *Leukemia* **34**, 3126–3135. https://doi.org/10.1038/s41375-020-01041-z (2020).
19. Alkhamis, T. M., Beissinger, R. L. & Chediak, J. R. Artificial surface effect on red blood cells and platelets in laminar shear flow. *Blood* **75**, 1568–1575 (1990).
20. Schwager, S. C. & Reinhart-King, C. A. Mechanobiology of microvesicle release, uptake, and microvesicle-mediated activation. *Curr. Top. Membr.* **86**, 255–278. https://doi.org/10.1016/bs.ctm.2020.08.004 (2020).
21. Raposo, G. & Stoorvogel, W. Extracellular vesicles: exosomes, microvesicles, and friends. *J. Cell Biol.* **200**, 373–383. https://doi.org/10.1083/jcb.201211138 (2013).
22. Chen, Y. T., Yuan, H. X., Ou, Z. J. & Ou, J. S. Microparticles (Exosomes) and atherosclerosis. *Curr. Atheroscler. Rep.* **22**, 23. https://doi.org/10.1007/s11883-020-00841-z (2020).
23. Porro, C., Trotta, T. & Panaro, M. A. Microvesicles in the brain: Biomarker, messenger or mediator? *J. Neuroimmunol.* **288**, 70–78. https://doi.org/10.1016/j.jneuroim.2015.09.006 (2015).
24. Tian, Y. et al. Brain-derived microparticles induce systemic coagulation in a murine model of traumatic brain injury. *Blood* **125**, 2151–2159. https://doi.org/10.1182/blood-2014-09-598805 (2015).
25. Zhao, Z. et al. Extracellular mitochondria released from traumatized brains induced platelet procoagulant activity. *Haematologica* **105**, 209–217. https://doi.org/10.3324/haematol.2018.214932 (2020).
26. Leitner, A. Enrichment strategies in phosphoproteomics. *Methods Mol. Biol. (Clifton N J).* **1355**, 105–121. https://doi.org/10.1007/978-1-4939-3049-4_7 (2016).
27. Zahedi, R. P., Begonja, A. J., Gambaryan, S. & Sickmann, A. Phosphoproteomics of human platelets: A quest for novel activation pathways. *Biochim. Biophys. Acta.* **1764**, 1963–1976. https://doi.org/10.1016/j.bbapap.2006.08.017 (2006).
28. Zhao, R. T. et al. Circular ribonucleic acid expression alteration in exosomes from the brain extracellular space after traumatic brain injury in mice. *J. Neurotrauma.* **35**, 2056–2066. https://doi.org/10.1089/neu.2017.5502 (2018).
29. Michelson, A. D. Flow cytometry: a clinical test of platelet function. *Blood* **87**, 4925–4936 (1996).
30. McEver, R. P. Selectin-carbohydrate interactions during inflammation and metastasis. *Glycoconj. J.* **14**, 585–591. https://doi.org/10.1023/a:1018584425879 (1997).
31. Serebruany, V. L., McKenzie, M. E., Levin, D. J. & Gurbel, P. A. Monitoring platelet Inhibition during chronic oral platelet glycoprotein IIb/IIIa blockade: are we missing something? *Thromb. Haemost.* **83**, 356–357 (2000).
32. Liu, X. et al. Use of non-contact hopping probe ion conductance microscopy to investigate dynamic morphology of live platelets. *Platelets* **26**, 480–485. https://doi.org/10.3109/09537104.2014.940888 (2015).
33. Cox, J. & Mann, M. MaxQuant enables high peptide identification rates, individualized p.p.b.-range mass accuracies and proteome-wide protein quantification. *Nat. Biotechnol.* **26**, 1367–1372. https://doi.org/10.1038/nbt.1511 (2008).
34. Cox, J. et al. Accurate proteome-wide label-free quantification by delayed normalization and maximal peptide ratio extraction, termed MaxLFQ. *Mol. Cell. Proteomics: MCP.* **13**, 2513–2526. https://doi.org/10.1074/mcp.M113.031591 (2014).
35. Ashburner, M. et al. Gene ontology: tool for the unification of biology. The gene ontology consortium. *Nat. Genet.* **25**, 25–29. https://doi.org/10.1038/75556 (2000).
36. Cheng, A., Grant, C. E., Noble, W. S. & Bailey, T. L. MoMo: discovery of statistically significant post-translational modification motifs. *Bioinf. (Oxford England).* **35**, 2774–2782. https://doi.org/10.1093/bioinformatics/bty1058 (2019).
37. Edbauer, D. et al. Identification and characterization of neuronal mitogen-activated protein kinase substrates using a specific phosphomotif antibody. *Mol. Cell. Proteomics: MCP.* **8**, 681–695. https://doi.org/10.1074/mcp.M800233-MCP200 (2009).
38. Seyfert, U. T., Haubelt, H., Vogt, A. & Hellstern, P. Variables influencing Multiplate(TM) whole blood impedance platelet aggregometry and turbidimetric platelet aggregation in healthy individuals. *Platelets* **18**, 199–206. https://doi.org/10.1080/09537100600944277 (2007).

39. Melki, I., Tessandier, N., Zufferey, A. & Boilard, E. Platelet microvesicles in health and disease. *Platelets* **28**, 214–221. https://doi.org/10.1080/09537104.2016.1265924 (2017).
40. Duchez, A. C. et al. Platelet microparticles are internalized in neutrophils via the concerted activity of 12-lipoxygenase and secreted phospholipase A2-IIA. *Proc. Natl. Acad. Sci. U.S.A.* **112**, E3564–3573. https://doi.org/10.1073/pnas.1507905112 (2015).
41. Vanhoutte, P. M. COX-1 and vascular disease. *Clin. Pharmacol. Ther.* **86**, 212–215. https://doi.org/10.1038/clpt.2009.108 (2009).
42. Vane, J. R., Bakhle, Y. S. & Botting, R. M. Cyclooxygenases 1 and 2. *Annu. Rev. Pharmacol. Toxicol.* **38**, 97–120. https://doi.org/10.1146/annurev.pharmtox.38.1.97 (1998).
43. Dec, K. et al. Long-term exposure to fluoride as a factor promoting changes in the expression and activity of cyclooxygenases (COX1 and COX2) in various rat brain structures. *Neurotoxicology* **74**, 81–90. https://doi.org/10.1016/j.neuro.2019.06.001 (2019).
44. Hankey, G. J. & Eikelboom, J. W. Aspirin resistance. *Lancet (London England)*. **367**, 606–617. https://doi.org/10.1016/s0140-6736(06)68040-9 (2006).
45. Macchi, L., Sorel, N. & Christiaens, L. Aspirin resistance: definitions, mechanisms, prevalence, and clinical significance. *Curr. Pharm. Des.* **12**, 251–258. https://doi.org/10.2174/138161206775193064 (2006).
46. Khismatullin, R. R. et al. Pathology of lung-specific thrombosis and inflammation in COVID-19. *J. Thromb. Haemostasis: JTH*. **19**, 3062–3072. https://doi.org/10.1111/jth.15532 (2021).
47. Denorme, F. & Campbell, R. A. Procoagulant platelets: novel players in thromboinflammation. *Am. J. Physiol. Cell Physiol.* **323**, C951–c958. https://doi.org/10.1152/ajpcell.00252.2022 (2022).
48. Kulkarni, P. P. & McCrae, K. R. Comprehensive analysis of procoagulant platelets exhibiting features of Necrosis, apoptosis and platelet activation. *J. Vis. Exp. JoVE*. https://doi.org/10.3791/68116 (2025).
49. Veuthey, L., Aliotta, A., Bertaggia Calderara, D., Pereira Portela, C. & Alberio, L. Mechanisms underlying dichotomous procoagulant COAT platelet Generation-A conceptual review summarizing current knowledge. *Int. J. Mol. Sci.* **23** https://doi.org/10.3390/ijms23052536 (2022).
50. Prus, G., Hoegl, A., Weinert, B. T. & Choudhary, C. Analysis and interpretation of protein Post-Translational modification site stoichiometry. *Trends Biochem. Sci.* **44**, 943–960. https://doi.org/10.1016/j.tibs.2019.06.003 (2019).
51. Cox, J. et al. Andromeda: a peptide search engine integrated into the MaxQuant environment. *J. Proteome Res.* **10**, 1794–1805. https://doi.org/10.1021/pr101065j (2011).
52. Lee, E. E., Winston-Gray, C., Barlow, J. W., Rissman, R. A. & Jeste, D. V. Plasma levels of neuron- and astrocyte-derived exosomal amyloid Beta1-42, amyloid Beta1-40, and phosphorylated Tau levels in schizophrenia patients and Non-psychiatric comparison subjects: relationships with cognitive functioning and psychopathology. *Front. Psychiatry*. **11**, 532624. https://doi.org/10.3389/fpsyt.2020.532624 (2020).
53. Küry, S. et al. De novo mutations in protein kinase genes CAMK2A and CAMK2B cause intellectual disability. *Am. J. Hum. Genet.* **101**, 768–788. https://doi.org/10.1016/j.ajhg.2017.10.003 (2017).
54. Bill, C. A. & Vines, C. M. Phospholipase C. *Adv. Exp. Med. Biol.* **1131**, 215–242. Doi:https://doi.org/10.1007/978-3-030-12457-1_9 (2020).
55. Stabel, S. & Parker, P. J. Protein kinase C. *Pharmacol. Ther.* **51**, 71–95. https://doi.org/10.1016/0163-7258(91)90042-k (1991).
56. Moore, D. T., Berger, B. W. & DeGrado, W. F. Protein-protein interactions in the membrane: sequence, structural, and biological motifs. *Structure (London, England)*. **16**, 991–1001. https://doi.org/10.1016/j.str.2008.05.007 (2008).
57. Ardito, F., Giuliani, M., Perrone, D., Troiano, G. & Lo Muzio, L. The crucial role of protein phosphorylation in cell signaling and its use as targeted therapy (Review). *Int. J. Mol. Med.* **40**, 271–280. https://doi.org/10.3892/ijmm.2017.3036 (2017).
58. Rubenstein, D. A. & Yin, W. Platelet-activation mechanisms and vascular remodeling. *Compr. Physiol.* **8**, 1117–1156. https://doi.org/10.1002/cphy.c170049 (2018).
59. Li, Z., Delaney, M. K., O'Brien, K. A. & Du, X. Signaling during platelet adhesion and activation. *Arterioscler. Thromb. Vasc. Biol.* **30**, 2341–2349. https://doi.org/10.1161/atvbaha.110.207522 (2010).

Author contributions

Y.H. performed the experiments, analyzed the data and wrote the paper; J.Z., Y.W., and X.L. participated in the execution of the experiment; R.Z. and Y.G. contributed to analysis and manuscript preparation; H.Y. and Y.T. contributed to the conception of the study. All authors read and approved the final manuscript.

Funding

This study was funded by major project of the Tianjin Natural Science Foundation (Tianjin Municipal Science and Technology Commission) (No. 21ZXJBSY00050) and the National Natural Science Foundation of China (No. 81971173 and 82371386).

Declarations

Competing interests

The authors declare no competing interests.

Additional information

Supplementary Information The online version contains supplementary material available at https://doi.org/10.1038/s41598-026-39509-0.

Correspondence and requests for materials should be addressed to H.-j.Y. or Y.T.